# Mechanism-based sirtuin enzyme activation

Xiangying Guan, Alok Upadhyay and Raj Chakrabarti*

*Division of Fundamental Research, PMC Advanced Technology, LLC, Mt. Laurel, NJ 08054*

## Abstract

Sirtuin enzymes are $NAD^+$-dependent protein deacylases that play a central role in the regulation of healthspan and lifespan in organisms ranging from yeast to mammals. There is intense interest in the activation of the seven mammalian sirtuins (SIRT1-7) in order to extend mammalian healthspan and lifespan. However, there is currently no understanding of how to design sirtuin-activating compounds beyond allosteric activators of SIRT1-catalyzed reactions that are limited to particular substrates. Moreover, across all families of enzymes, only a dozen or so distinct classes of non-natural small molecule activators have been characterized, with only four known modes of activation among them. None of these modes of activation are based on the unique catalytic reaction mechanisms of the target enzymes. Here, we report a general mode of sirtuin activation that is distinct from any of the known modes of enzyme activation. Based on the conserved mechanism of sirtuin-catalyzed deacylation reactions, we establish biophysical properties of small molecule modulators that can result in enzyme activation for any sirtuin and any substrate. Building upon this framework, we propose mechanism-based workflows for the design of new sirtuin-activating compounds. We demonstrate experimentally the existence of small molecule modulators that activate multiple sirtuins through the proposed mode of action.

## Significance Statement

Compared to enzyme inhibitors, which constitute the vast majority of today's drugs, enzyme activators have considerable advantages. However, they are much more difficult to design, because enzymatic catalysis has been optimized over billions of years of evolution. Sirtuin-activating compounds (STACs) are enzyme activators that can extend mammalian healthspan and lifespan. Unfortunately, the only known mode of STAC action is limited to accelerating selected functions of a single mammalian sirtuin enzyme. Here, we report a wholly new mode of enzyme activation that exploits the common catalytic mechanism of all sirtuin enzymes, hence being applicable to any function of any sirtuin. This discovery expands our understanding of enzyme activation, and lays the foundation for development of a new generation of drugs for mammalian healthspan and lifespan extension.

* To whom correspondence should be addressed:

Raj Chakrabarti, Ph.D.
Division of Fundamental Research
PMC Advanced Technology, LLC
1288 Route 73 South
Mt. Laurel, NJ 08054, USA
Phone: (609) 216-4644
Email: raj@pmc-group.com

## Introduction

Sirtuin (silent information regulator) enzymes, which catalyze $NAD^+$-dependent protein post-translational modifications, have emerged as critical regulators of many cellular pathways. In particular, these enzymes protect against age-related diseases and serve as key mediators of longevity in evolutionarily distant organismic models [1]. Sirtuins are $NAD^+$-dependent lysine deacylases, requiring the cofactor $NAD^+$ to cleave acyl groups from lysine side chains of their substrate proteins, and producing nicotinamide (NAM) as a by-product. A thorough understanding of sirtuin chemistry is not only of fundamental importance, but also of considerable medicinal importance, since there is enormous current interest in the development of new mechanism-based sirtuin modulators [2, 3]. The mechanism of sirtuin-catalyzed, $NAD^+$-dependent protein deacylation is depicted in Fig. 1 [4-6].

Recently, in order to extend mammalian healthspan and lifespan, intense interest has developed in the activation of the seven mammalian sirtuin enzymes (SIRT1-7). Prior work on sirtuin activation has relied exclusively on experimental screening, with an emphasis on allosteric activation of the SIRT1 enzyme. Indeed, small molecule allosteric activators of SIRT1 have been demonstrated to induce lifespan extension in model organisms such as mice [7, 8]. Allosteric activation is one of four known modes by which small molecules can activate enzymes [9]. Allosteric activators most commonly function by decreasing the dissociation constant for the substrate (the acylated protein dissociation constant $K_{d,Ac-\mathrm{Pr}}$ in the case of sirtuins).

Nearly all known sirtuin activators allosterically target SIRT1 and bind outside of the active site to an allosteric domain in SIRT1 that is not shared by SIRT2-7 [10]. Moreover, allosteric activators only work with a limited set of SIRT1 substrates [11-13]. It is now known that other sirtuins -- including SIRT2, SIRT3 and SIRT6 -- and multiple protein substrates play significant roles in regulating mammalian longevity [14-16]. General strategies for the activation of any mammalian sirtuin (including activation of SIRT1 for other substrates) are hence of central importance, but not understood. In general, allosteric activation to decrease substrate $K_d$ will not be an option for enzyme activation, rendering mechanism-based activation essential.

Foundations for the rational design of mechanism-based sirtuin activators have been lacking, partly due to the absence of a clear understanding of the kinetics of sirtuin-catalyzed deacylation. Several types of mechanism-based sirtuin inhibitors have been reported recently in the literature, including Ex-527 and Sir-Real2 [17, 18]. However, mechanism-based activation has proven far more elusive, due to the difficulty in screening for the balance of properties needed for a modulator to have the net effect of accelerating catalytic turnover. While there are many ways to inhibit an enzyme's mechanism, there are far fewer ways to activate it. These efforts have been hindered by the lack of a complete steady state kinetic model of sirtuin catalysis that accounts for the effects of both $NAD^+$ and NAM on activity.

In the so-called "$NAD^+$ world" picture of global metabolic regulation, the intracellular concentrations of the sirtuin cofactor $NAD^+$, which can decrease with age, play a central role in regulating mammalian metabolism and health through sirtuin-dependent pathways [19]. Due to the comparatively high Michaelis constants for $NAD^+$ ($K_{m,NAD+}$'s) of mammalian sirtuins, their activities are sensitive to intracellular $NAD^+$ levels [4, 20]. The systemic decrease in $NAD^+$ levels that accompanies organismic aging downregulates sirtuin activity and has been identified as a central factor leading to various types of age-related health decline [21, 22], whereas increases in $NAD^+$ levels can upregulate sirtuin activity and as a result mitigate or even reverse several aspects of this decline [19, 23].

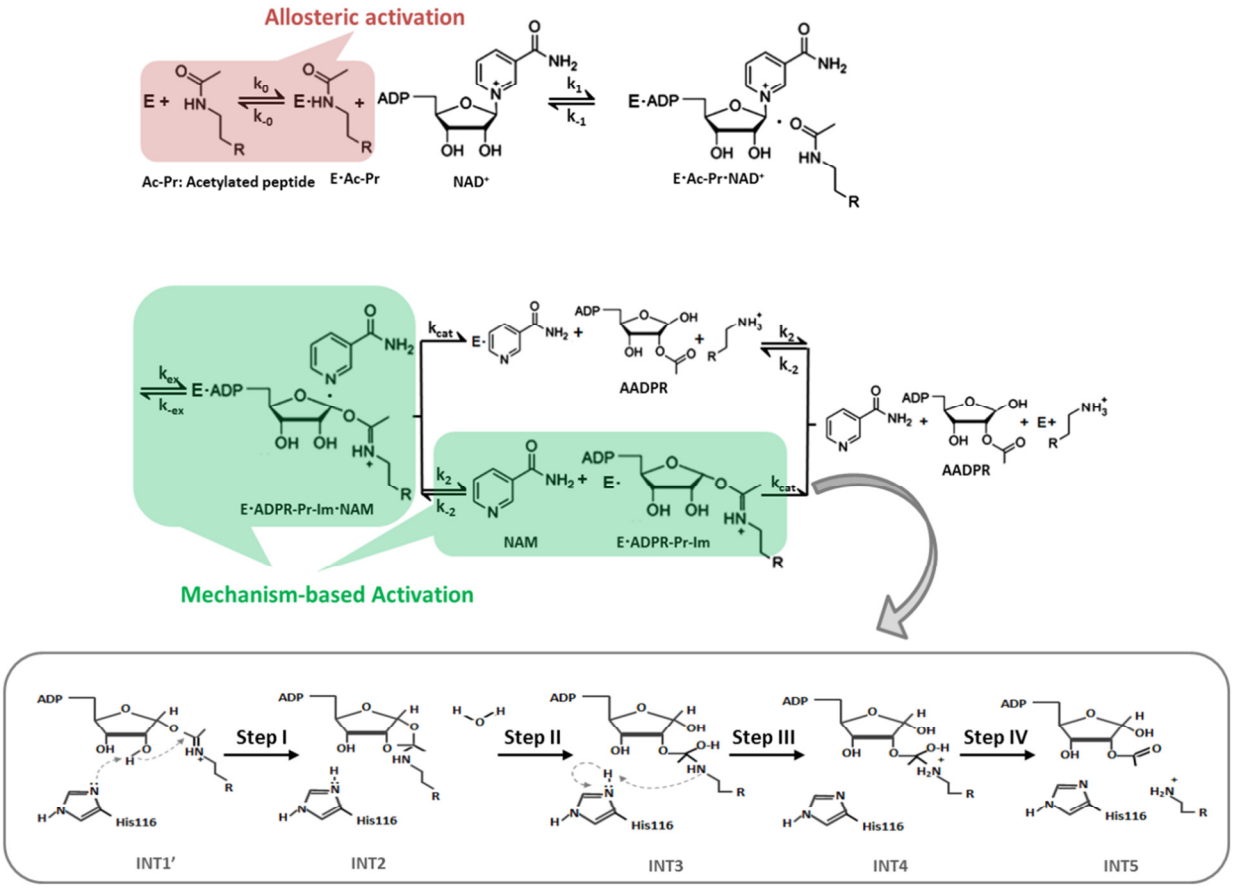


**Figure 1. Chemical mechanism of sirtuin-catalyzed deacylation and modes of sirtuin activation.** Following sequential binding of acylated peptide substrate and $NAD^+$ cofactor, the reaction proceeds in two consecutive stages: i) cleavage of the nicotinamide moiety of $NAD^+$ (ADP-ribosyl transfer) through the nucleophilic attack of the acetyl-Lys side chain of the protein substrate to form a positively charged O-alkylimidate intermediate, and ii) subsequent formation of deacylated peptide. For simplicity, all steps of stage ii as well as AADPR + Pr dissociation are depicted to occur together with rate limiting constant $k_{cat}$ . **Red**: Allosteric activation increases the affinity of a limited set of peptide substrates for the SIRT1 enzyme only and requires an allosteric binding site. **Green**: Mechanism-based activation is a new mode of enzyme activation that relies on the conserved sirtuin reaction mechanism rather than an increase in the affinity of selected peptide substrates.

As such, NAD+ supplementation has emerged as a promising alternative to allosteric activation of sirtuins [23]. Unlike allosteric activators like resveratrol, which are SIRT1-specific and have not been successfully applied to other sirtuins [10], $NAD^+$ supplementation can activate most mammalian sirtuins in a substrate-independent fashion. Moreover, allosteric activators cannot fully compensate for the reduction in sirtuin activity that occurs through $NAD^+$ decline during aging. On the other hand, the effects of $NAD^+$ supplementation are not specific to sirtuins and prohibitively high concentrations of $NAD^+$, along with associated undesirable side effects, may be required to elicit the increases in sirtuin activity required to combat age-related diseases.

A preferred general strategy for activation of sirtuins (Fig. 1) would be to increase their sensitivity to $NAD^+$ through a reduction of $K_{m,NAD+}$. $K_{m,NAD+}$ reduction would have a similar activating effect to $NAD^+$

supplementation, but would be selective for sirtuins and could potentially even provide isoform specific sirtuin activation. Importantly, due to the sirtuin nicotinamide cleavage reaction that involves the $NAD^+$ cofactor, modulation of $K_{m,NAD+}$ may in principle be achievable by means other than altering the binding affinity of $NAD^+$. Unlike allosteric activation that reduces $K_{d,Ac-\mathrm{Pr}}$, this approach would be applicable to any sirtuin and any substrate.

In this paper, we present a general framework for activation of sirtuin enzymes that is distinct from any of the known modes of enzyme activation, based on the fundamental mechanism of the sirtuin deacylation reaction. We first introduce a steady-state model of sirtuin-catalyzed deacylation reactions in the presence of $NAD^+$ cofactor and endogenous inhibitor NAM, and then establish quantitatively how $K_{m,NAD+}$ can be modified by small molecules, identifying the biophysical properties that small molecules must have to function as such mechanism-based activators. We propose workflows suitable for mechanism-based design of sirtuin activating compounds and present experimental evidence for the existence of mechanism-based sirtuin activating compounds (MB-STACs) that operate according to the mechanisms presented.

## Results

### *Steady-state sirtuin kinetic modeling*

To a greater extent than inhibitor design, rational activator design requires the use of a mechanistic model in the workflow. In this section we develop a steady state model for sirtuin-catalyzed deacylation that is suitable for a) investigation of the mode of action of mechanism-based sirtuin modulators, including activators; b) design of mechanism-based sirtuin activating compounds. We first summarize the state of knowledge regarding the sirtuin-catalyzed deacylation mechanism.

The sirtuin catalytic cycle (Fig. 1) is believed to proceed in two consecutive stages [4]. The initial stage (ADP-ribosylation) involves the cleavage of the nicotinamide moiety of $NAD^+$ and the nucleophilic attack of the acyl-Lys side chain of the protein substrate to form a positively charged O-alkylimidate intermediate [4, 24]. Nicotinamide-induced reversal of the intermediate (the so-called base exchange reaction) causes reformation of $NAD^+$ and acyl-Lys protein. The energetics of this reversible reaction affects both the potency of NAM inhibition of sirtuins and the Michaelis constant for NAD+ ($K_{m,NAD+}$). The second stage of sirtuin catalysis, which includes the rate-determining step, involves four successive steps that culminate in deacylation of the Lys side chain of the protein substrate and the formation of O-acetyl ADP ribose coproduct [4, 6, 25].

A tractable steady state model suitable for the purpose of mechanism-based sirtuin activator design must account for the following important features:

- The calculated free energy of activation for nicotinamide cleavage (ADP -ribosylation of the acyl-Lys substrate) in the bacterial sirtuin enzyme Sir2Tm as computed through mixed quantum/molecular mechanics (QM/MM) methods is 15.7 kcal $mol^{-1}$ [5, 26]. An experimental value of 16.4 kcal $mol^{-1}$ for the activation barrier in the yeast sirtuin homolog Hst2 was estimated from the reaction rate 6.7 $s^{-1}$ of nicotinamide formation. The nicotinamide cleavage reaction is endothermic, with a computed $\Delta G$ of 4.98 kcal $mol^{-1}$ in Sir2Tm [26].

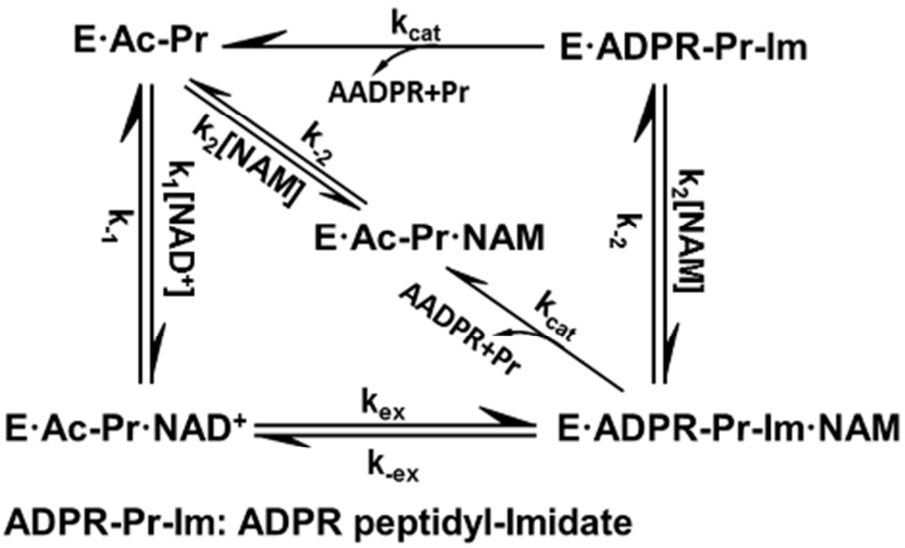


**Figure 2. General model for sirtuin-catalyzed deacylation in the presence of $NAD^+$ and NAM.** This model, based on the reaction mechanism depicted in Fig. 1, provides a minimal kinetic model that captures the essential features of sirtuin deacylation kinetics suitable for predicting the effects of mechanism-based modulators on sirtuin activity. In the presence of saturating Ac-Pr, E is rapidly converted into E·Ac-Pr and NAM binding to E can be neglected, resulting in a simplified reaction network with 5 species. Ac-Pr, acetylated peptide; ADPR, adenosine diphosphate ribose; AADPR, O-acetyl adenosine diphosphate ribose.

- The calculated free energy of activation for the rate limiting chemistry step (collapse of the bicyclic intermediate) from QM/MM simulations is 19.2 kcal $mol^{-1}$ for Sir2Tm [27], in good agreement with the experimental value of 18.6 kcal/$mol^{-1}$ estimated from the $k_{cat}$ value of 0.170 ± 0.006 $s^{-1}$ [28] (0.2 +/- 0.03 $s^{-1}$ for Hst2 [24]).

- The remaining steps in the catalytic cycle are significantly faster than the above steps. The other chemistry steps in stage 2 of the reaction are effectively irreversible [27], as is product release in the presence of saturating peptide concentrations.

We hence include in our kinetic model representations of all steps in stage 1 of the reaction, including the nicotinamide cleavage/base exchange and nicotinamide binding steps. However, for simplicity, we do not include in the present model a representation of each of the individual chemistry steps in stage 2 of the reaction or final product release, instead subsuming these steps under the smallest rate constant, which we call $k_{cat}$. Since all these steps are effectively irreversible, the full steady state model including these steps can be immediately derived from the basic model through simple modifications, to be described in a subsequent revision, that are not essential to the analysis of mechanism-based activation. The above observations motivate the kinetic model represented in Fig. 2 [29]. This Figure shows a general reaction scheme for sirtuin deacylation including base exchange inhibition.

The reaction mechanism of sirtuins precludes the use of rapid equilibrium methods for the derivation of even an approximate initial rate model; steady-state modeling is essential. The rate equations for the

reaction network in Fig. 2 enable the derivation of steady-state conditions for the reaction. Solving the linear system of algebraic steady-state equations and mass balance constraints for the concentrations

$$[\mathrm{E.Ac-Pr}],[E.\mathrm{Ac-Pr.NAD^+}],[E.ADPR-Ac-\mathrm{Im.NAM}],[E.\mathrm{ADPR}-Ac-\mathrm{Im}],[E.NAM]$$

in terms of the rate constants and [NAD+],[NAM], which are assumed to be in significant excess and hence approximately equal to their initial concentrations $[\mathrm{NAD+}]_0$,$[\mathrm{NAM}]_0$ respectively, we obtain expressions of the form (1):

$$\begin{aligned}
&[E.Ac-\mathrm{Pr}]/[E]_0 = c_{11}+c_{12}[\mathrm{NAM}]\\
&[E.Ac-\mathrm{Pr.NAD^+}]/[E]_0 = c_{21}[NAD^+]+c_{22}[\mathrm{NAD^+}][\mathrm{NAM}]\\
&[E.ADPR-Ac-\mathrm{Im}.NAM]/[E]_0 = c_{31}[NAD^+]+c_{32}[NAD^+][NAM] \qquad (1)\\
&[E.ADPR-Ac-\mathrm{Im}]/[E]_0 = c_{41}[\mathrm{NAD^+}]\\
&[E.\mathrm{Ac-Pr}.NAM]/[E]_0 = c_{51}[NAD^+]+c_{52}[NAM]+\mathrm{c}_{53}[\mathrm{NAD^+}][\mathrm{NAM}]+\mathrm{c}_{54}[NAM]^2
\end{aligned}$$

where the term $c_{54}$ that is second order in [NAM] will be omitted from the analysis below. Expressions for the $c_{ij}$'sare provided in the Appendix. The initial rate of deacylation can be then expressed

$$\frac{v}{v_{\max}} = \frac{[\mathrm{NAD^+}]\left(1+\frac{[\mathrm{NAM}]}{K_1}\right)}{K_{m,\mathrm{NAD^+}}\left(1+\frac{[\mathrm{NAM}]}{K_2}\right)+[\mathrm{NAD^+}]\left(1+\frac{[\mathrm{NAM}]}{K_3}\right)} \qquad (2)$$

with

$$v_{\max} = \frac{k_{cat} * \mathrm{k_1 k_{ex} k_{-2}} \left(k_{-2} + k_{cat}\right)}{k_{-2}k_1k_{ex}k_{-2} + k_{cat}\left(k_{-2}k_{cat}k_1 + k_{-2}k_{-2}k_1 + k_{-2}k_1k_{-ex} + k_{-2}k_1k_{ex} + k_1k_{ex}k_{cat}\right)}[E]_0$$
$$\approx k_{cat}[E]_0$$

$$K_{m,NAD^+} = \frac{k_{cat}k_{-2}\left[k_{ex}k_{cat} + k_{-1}k_{cat} + k_{ex}k_{-2} + k_{-1}k_{-2} + k_{-ex}k_{-1}\right]}{k_{-2}k_1k_{ex}k_{-2} + k_{cat}\left(k_{-2}k_{cat}k_1 + k_{-2}k_{-2}k_1 + k_{-2}k_1k_{-ex} + k_{-2}k_1k_{ex} + k_1k_{ex}k_{cat}\right)}$$
$$\approx k_{cat}\frac{k_{ex}k_{-2} + k_{-1}\left(k_{-2} + k_{-ex}\right)}{k_1k_{ex}k_{-2}} = k_{cat}\left(\frac{1}{k_1} + K_{d,NAD+}\frac{k_{-2} + k_{-ex}}{k_{-2}k_{ex}}\right)$$

$$\frac{1}{K_1} = \frac{k_2}{k_{-2} + k_{cat}} \approx \frac{1}{K_{d,NAM}} \qquad (3a-e)$$

$$\frac{1}{K_2} = \frac{1}{K_{m,\mathrm{NAD^+}}}\frac{k_2k_{-ex}k_{-1}k_{-2} + k_{cat}\left(k_2k_{ex}k_{cat} + k_{-1}k_2k_{cat} + k_{-ex}k_{-1}k_2 + 2k_{-2}k_2k_{ex} + 2k_{-2}k_2k_{-1}\right)}{k_{-2}k_1k_{ex}k_{-2} + k_{cat}\left(k_{-2}k_{cat}k_1 + k_{-2}k_{-2}k_1 + k_{-2}k_1k_{-ex} + k_{-2}k_1k_{ex} + k_1k_{ex}k_{cat}\right)} \approx \frac{K_{d,NAD^+}K_{ex}}{K_{m,\mathrm{NAD^+}}K_{d,NAM}}$$

$$\frac{1}{K_3} \triangleq \frac{1}{\alpha K_2} = \frac{k_1k_2k_{-2}\left(k_{-ex} + k_{ex}\right) + k_{cat}k_1k_2\left(k_{-2} + k_{ex}\right)}{k_1k_{-2}k_{-2}k_{ex} + k_{cat}\left(k_{-2}k_{cat}k_1 + k_{-2}k_{-2}k_1 + k_{-2}k_1k_{-ex} + k_{-2}k_1k_{ex} + k_1k_{ex}k_{cat}\right)} \approx \frac{1 + K_{ex}}{K_{d,NAM}}$$

where $K_{ex} \equiv k_{-ex}/k_{ex}$ and the approximations refer to the case where $k_{cat} \ll k_j,\ j \neq cat$. The quality of this approximation can be assessed for the chemistry steps based on QM/MM simulation data, which was cited above for yeast and bacterial sirtuins.

Equation (2) is typically represented graphically in terms of either double reciprocal plots at constant [NAM] or Dixon plots at constant [NAD+]. In the former case, the slope of the plot (1/v vs 1/[NAD+]) at [NAM]=0 is $\frac{K_{m,NAD^+}}{v_{\max}}$, for which the expression is:

$$\frac{K_{m,NAD^+}}{v_{\max}} \approx \frac{1}{[E]_0}\left(\frac{1}{k_1} + K_{d,NAD+}\frac{k_{-2} + k_{-ex}}{k_{-2}k_{ex}}\right) \approx \frac{K_{m,NAD^+}}{k_{cat}[E]_0} \qquad (4)$$

whereas for the Dixon plot, the expression for the slope at 1/[NAD+]=0 is approximately [29]:

$$\frac{1}{K_3}\frac{1}{v_{max}} \approx \frac{1 + K_{ex}}{K_{d,NAM}}\ \frac{1}{k_{cat}[E]_0}. \qquad (5)$$

The steady state parameter $\alpha$ in equation (3e), which is a measure of the extent of competitive inhibition by the endogeneous inhibitor NAM against the cofactor NAD+, can be expressed in terms of the ratio of $K_{d,NAD+}$ and $K_{m,NAD+}$ [29]:

$$\alpha = \frac{K_3}{K_2} \approx \frac{K_{d,NAD+}}{K_{m,NAD+}} \frac{K_{ex}}{1+K_{ex}} \quad (6)$$

which, together with expression (3b) for $K_{m,NAD+}$, demonstrates how the kinetics of inhibition of deacylation by NAM can reveal differences in $NAD^+$ binding affinity and nicotinamide cleavage rates among sirtuins. The origins of different NAD+ binding affinities among sirtuins were studied structurally and computationally in [29]. Given that $K_{ex}$ is generally >> 1 for sirtuins, it is apparent from eqn (6) that the difference in magnitudes of $K_{d,NAD+}$ and $K_{m,NAD+}$ for sirtuins is captured by $\alpha$. $K_{m,NAD+}$, not $K_{d,NAD+}$ alone, determines the sensitivity of sirtuin activity to NAD+, and can vary across this family of enzymes. The initial rate model and the definition of $\alpha$ allow $K_{d,NAD+}$ to be estimated (under suitable approximations) by steady state deacylation experiments that vary [NAM] as well as [NAD+].

In addition to the approximation $k_{cat} \ll k_j,\ j \neq cat$, several experimental observations can further simplify the form of the expressions (4) for the sirtuin steady state constants. First, we assume $k_{-2} >> k_j,\ j \neq -2$ based on viscosity measurements that suggest NAM dissociates rapidly following cleavage [30]. Under this approximation, the expression for $K_{m,NAD+}$ becomes:

$$K_{m,NAD+} \approx k_{cat}\left(\frac{1}{k_1} + \frac{K_{d,NAD+}}{k_{ex}}\right) \quad (7)$$

The magnitudes of the on/off rates for NAD+ binding also affect the accuracy of approximations to equations (2,3). Such approximations will be studied in greater detail in a subsequent work.

As can be seen from eqn (3b), the kinetics of the nicotinamide cleavage reaction and the rate limiting step of deacylation both play essential roles in determining the value of $K_{m,NAD+}$. Note that in rapid equilibrium models of enzyme kinetics, which are not applicable to sirtuins, $K_m \approx K_d$. The difference between $K_{d,NAD+}$ and $K_{m,NAD+}$ has important implications for mechanism-based activation of sirtuins by small molecules [29]. In particular, as we will show in this work, decrease of $K_{m,NAD+}$ independently of $K_{d,NAD+}$ can increase the activity of sirtuins at [NAM]=0. The kinetic model above establishes foundations for how this can be done.

*Mechanism-based sirtuin activation*

Previous attempts to develop a general approach to sirtuin activation [30, 31] only considered competitive inhibitors of base exchange, which cannot activate in the absence of NAM. This is not actually a form of enzyme activation, but rather derepression of inhibition. By contrast, here we present paradigms and design criteria for activation of sirtuins in either the absence or presence of NAM. Based on expression (3b) for $K_{m,NAD+}$, it is in principle possible to activate sirtuins (not just SIRT1) for any substrate by alteration of rate constants in the reaction mechanism other than $k_1$,$k_{-1}$ and $k_{cat}$, so as to reduce $K_{m,NAD+}$ -- not $K_{d,Ac\text{-}Pr}$ as with allosteric activators, which increase the peptide binding affinity of SIRT1 in a substrate-dependent fashion. We now explore how this may be achieved by augmenting the kinetic model to include putative mechanism-based activators (A) that can bind simultaneously with NAD+ and NAM. Fig. 3 depicts the reaction diagram for mechanism-based activation of sirtuins. Note that only the top and

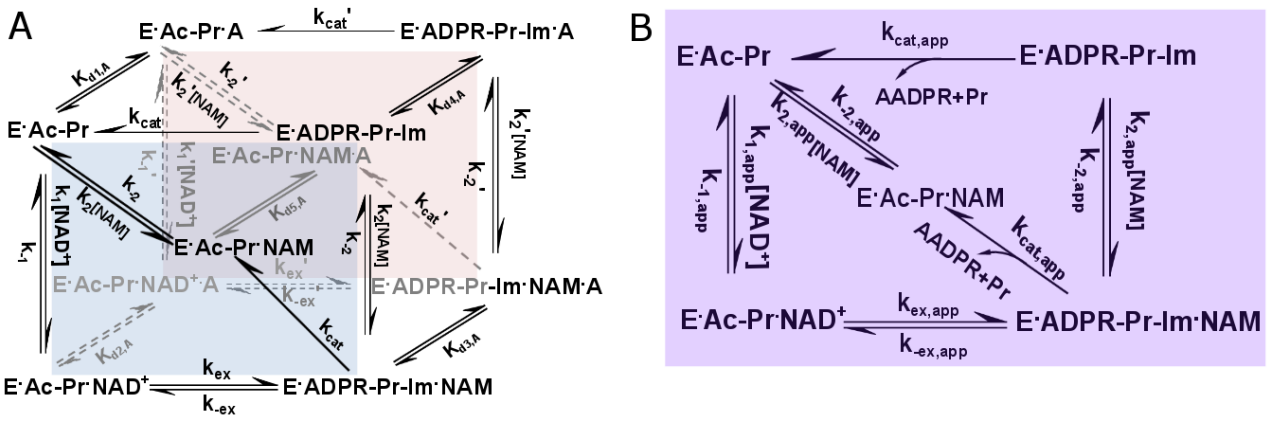


**Figure 3. General model for mechanism-based sirtuin enzyme activation.** A) The front face of the cube (blue) depicts the salient steps of the sirtuin reaction network in the absence of bound modulator. The back face of the cube (red) depicts the reaction network in the presence of bound modulator (denoted by "A"). Each rate constant depicted on the front face has an associated modulated value on the back face, designated with a prime, that is a consequence of modulator binding. B) The purple face is the apparent reaction network in the presence of a nonsaturating concentration of modulator.

front faces of this cube are relevant to the mechanism of action of the previously proposed competitive inhibitors of base exchange [30, 31].

At any [A] there exist apparent values of each of the rate constants in the sirtuin reaction mechanism. These are denoted by "app" in the Figure. There are also corresponding "app" values of the steady state, Michaelis, and dissociation constants in equation (3). Moreover, at saturating [A] of a known activator, the modulated equilibrium and dissociation constants (which do not depend on determination of steady state species concentrations) can be estimated with only deacylation experiments according to the theory presented above. The exchange equilibrium constant $K_{ex}'$ and NAD+,NAM dissociation constants $K_{d,NAD+}'$ $K_{d,NAM}'$ in the presence of A are related to their original values as follows:

$$\mathrm{K_{d,NAD+}}' = K_{d,NAD+}\frac{K_{d2,A}}{K_{d1,A}};\quad K_{ex}' = K_{ex}\frac{K_{d3,A}}{K_{d2,A}};\quad K_{d,NAM}' = K_{d,NAM}\frac{K_{d3,A}}{K_{d4,A}} \qquad (8)$$

where the $K_{d,A}$'s are the dissociation constants for A depicted in Fig. 3.

In order to predict the effect on $K_{m,NAD^+,app}$ of a modulator with specified relative binding affinities for the complexes in the sirtuin reaction mechanism, it is important to develop a model that is capable of quantifying, under suitable approximations, the effect of such a modulator on the apparent steady state parameters of the enzyme. Since the full steady state expression relating the original to the apparent rate constants has many terms containing products of additional side and back face rate constants, we use a rapid equilibrium segments approach to arrive at simple definitions of the apparent Michaelis constant and other steady state constants for the reaction in terms of the original expressions for these constants and the dissociation constants for binding of A to the various complexes in the sirtuin reaction mechanism. This provides a minimal model with the least number of additional parameters required to model sirtuin activation mechanisms. In our treatment, we will assume that rapid equilibrium applies on

both the side faces and the back face. Under this approximation, at low [A] the expressions for the induced changes in each of the rate constant products appearing in the coefficients $c_{ij}$ and $c_{i'j'}$, i'=i of equation (1) (see Appendix for expressions for these products) are the same and linear in [A]. For example, in the case of $E.Ac-\Pr$, the steady state species concentrations become:

$$\begin{aligned}&[E.Ac-\Pr]/[E.Ac-\Pr]_0 \approx c_{11}+c_{12}[\mathrm{NAM}]\\&[E.Ac-\Pr.\mathrm{A}]/[E.Ac-\Pr]_0 \approx \frac{[A]}{K_{d1,A}}\left(c_{11}+c_{12}[\mathrm{NAM}]\right)\end{aligned} \tag{9}$$

The rapid equilibrium segments expressions for all species concentrations in equation (1) in the presence of A are provided in the Appendix.

Expressions for apparent values of all steady state parameters introduced in equation (3) (i.e., modulated versions of constants $v_{\max,}, K_{m,NAD+,}K_1, K_{2,} K_3$) in the presence of a given [A] can now be derived. In the following, several types of approximations will be invoked:

i: rapid equilibrium segments approximation
ii: $k_{cat}(1+K_{dl,A}) \ll k_j(1+K_{dl',A}),\ j\neq cat,\ l=1,...,5$
iii: $k_{-2}(1+K_{dl,A}) \gg k_j(1+K_{dl',A}),\ j\neq -2,\ l=1,...,5$ (rapid NAM dissociation)

- $\frac{v_{\max,\mathrm{app}}}{[E]_0}$:

$$\frac{v_{\max,\mathrm{app}}}{[E]_0}=\frac{k_{cat,\mathrm{app}}\left(c_{31,app}+c_{41,app}\right)}{c_{21,app}+c_{31,app}+c_{41,app}+c_{51,app}}$$

$$\approx\frac{k_{cat}\left(k_{cat}k_1k_{ex}k_{-2}\left(1+[A]/K_{d3,A}\right)+k_1k_{ex}k_{-2}k_{-2}\left(1+[A]/K_{d4,A}\right)\right)}{k_{cat}\left(k_{-2}k_1k_{cat}+k_{-2}k_1k_{-2}+k_{-2}k_1k_{-ex}\right)\left(1+[A]/K_{d2,A}\right)+k_{cat}k_1k_{ex}k_{-2}\left(1+[A]/K_{d3,A}\right)+k_1k_{ex}k_{-2}k_{-2}\left(1+[A]/K_{d4,A}\right)+k_{cat}k_1k_{ex}k_{cat}\left(1+[A]/K_{d5,A}\right)}$$

$$\approx\frac{k_{cat}c_{41}\left(1+[A]/K_{dA,4}\right)}{c_{41}\left(1+[A]/K_{dA,4}\right)}=k_{cat}\approx k_{cat,app} \tag{10}$$

- $K_{m,NAD^+,app}$:

$$K_{m,NAD^+,app} = \frac{c_{11,app}}{c_{21,app} + c_{31,app} + c_{41,app} + c_{51,app}}$$

$$\approx \frac{c_{11}\left(1+\frac{[A]}{K_{d1,A}}\right)}{c_{21}\left(1+\frac{[A]}{K_{d2,A}}\right)+c_{31}\left(1+\frac{[A]}{K_{d3,A}}\right)+c_{41}\left(1+\frac{[A]}{K_{d4,A}}\right)+c_{51}\left(1+\frac{[A]}{K_{d5,A}}\right)}$$

$$\approx k_{cat}\left(\frac{1}{k_1}+\frac{K_{d,NAD+}}{k_{ex}}\right)\frac{1+[A]/K_{d1,A}}{1+[A]/K_{d4,A}} \approx k_{cat,app}\left(\frac{1}{k_1}+\frac{K_{d,NAD+,app}}{k_{ex}\frac{1+[A]/K_{d2,A}}{1+[A]/K_{d1,A}}}\right)\frac{1+[A]/K_{d1,A}}{1+[A]/K_{d4,A}} \quad (11)$$

$$\approx k_{cat,app}\left(\frac{1}{k_{1,app}}+\frac{K_{d,NAD+,app}}{k_{ex,app}}\right)$$

- $\alpha_{app}$ and $\alpha_{app}K_{m,NAD+,app}$:

Recall that $\alpha$ provides an estimate of the ratio of the dissociation and Michaelis constants for $NAD^+$.

$$\alpha_{app} \approx \frac{c_{12}\left(1+[A]/K_{d1,A}\right)+c_{52}\left(1+[A]/K_{d5,A}\right)}{c_{22}\left(1+[A]/K_{d2,A}\right)+c_{32}\left(1+[A]/K_{d3,A}\right)+c_{53}\left(1+[A]/K_{d5,A}\right)}\frac{1}{K_{m,NAD+,app}} \quad (12)$$

$$\approx \frac{K_{d,NAD+}}{K_{m,NAD+}}\frac{K_{ex}}{1+K_{ex}}\frac{\left(1+[A]/K_{d4,A}\right)}{\left(1+[A]/K_{d2,A}\right)} \approx \frac{K_{d,NAD+,app}}{K_{m,NAD+,app}}\frac{K_{ex,app}}{1+K_{ex,app}}$$

$$\alpha_{app}K_{m,NAD+,app} \approx K_{d,NAD+}\frac{K_{ex}}{1+K_{ex}}\frac{\left(1+[A]/K_{d1,A}\right)}{\left(1+[A]/K_{d2,A}\right)} \approx K_{d,NAD+,app}\frac{K_{ex,app}}{1+K_{ex,app}} \quad (13)$$

The latter provides an estimate of $K_{d,NAD+,app}$ if $K_{ex} \gg 1$, as it is believed to be for most sirtuins.

- $K_{3,app}$:

Under approximation (ii), $K_3$ isolates nicotinamide cleavage / base exchange-specific effects.

$$\frac{1}{K_{3,app}} \approx \frac{c_{22}\left(1+[A]/K_{d2,A}\right)+c_{32}(1+[A]/K_{d3,A})+c_{53}(1+[A]/K_{d5,A})}{c_{21}\left(1+[A]/K_{d2,A}\right)+c_{31}(1+[A]/K_{d3,A})+c_{41}(1+[A]/K_{d4,A})+c_{51}(1+/K_{d5,A})}$$
$$\approx \frac{1+K_{ex}}{K_{d,NAM}}\frac{\left(1+[A]/K_{d2,A}\right)}{(1+[A]/K_{d4,A})} \approx \frac{1+K_{ex,app}}{K_{d,NAM,app}} \qquad (14)$$

- $K_{2,app}$:

$$\frac{1}{K_{2,app}} = \frac{c_{12,app}+c_{52,app}}{c_{11,app}} \approx \frac{c_{12}\left(1+[A]/K_{d1,A}\right)+c_{52}\left(1+[A]/K_{d5,A}\right)}{c_{11}\left(1+[A]/K_{d1,A}\right)}$$
$$\approx \frac{c_{12}\left(1+[A]/K_{d1,A}\right)}{c_{11}\left(1+[A]/K_{d1,A}\right)} = \frac{K_{d,NAD^+}K_{ex}}{K_{m,\mathrm{NAD}^+}K_{d,NAM}} \approx \frac{K_{d,NAD^+,app}K_{ex,app}}{K_{m,\mathrm{NAD}^+,app}K_{d,NAM,app}} \qquad (15)$$

Regarding the quality of the approximations in this case, note from (15) and (A1) that unlike any of the other steady-state parameters, the modulation $\frac{1}{K_{2,app}}-\frac{1}{K_2}$ induced by [A] is proportional to $k_{cat}$ under the rapid equilibrium segments approximation (first approximation above). Hence, if one is interested in estimating the sign of this modulation, the small $k_{cat}$ approximation (second approximation above) should not be applied. Also, under the rapid equilibrium segments approximation, $K_{2,app}$ is the only constant that relies on a ratio of two $c_{ij}$'s with $i'=i,\ j'\neq j$, and hence the ratio of the same factor in [A]. It is obvious that the apparent values of rate constant products in the numerator and denominator above cannot be precisely equal and hence $K_{2,app}$ will have to change slightly from $K_2$.

- $K_{1,app}$:

$$\frac{1}{K_{1,app}} = \frac{c_{32,app}}{c_{31,app} + c_{42,app}}$$

$$\approx \frac{k_1 k_{ex} k_2 k_{-2} \left(1 + [A]/K_{d3,A}\right)}{k_{cat} k_1 k_{ex} k_{-2} (1 + [A]/K_{d3,A}) + k_1 k_{ex} k_{-2} k_{-2} (1 + [A]/K_{d4,A})}$$

$$\approx \frac{1}{K_{d,NAM}} \frac{1 + [A]/K_{d3,A}}{1 + [A]/K_{d4,A}} \qquad (16)$$

*Conditions for mechanism-based activation*

We now consider thermodynamic conditions on the binding of a modulator A for mechanism-based sirtuin activation under the rapid equilibrium segments approximation, along with the expected changes in the steady state, equilibrium and dissociation constants in the sirtuin reaction mechanism.

First, according to equation (10), $\frac{v_{\max}}{[E]_0}$ is roughly unchanged within this family of mechanisms as long as the $K_{d,A}$'s for [A] binding to the various represented complexes in the reaction mechanism satisfy condition (iii). Thus, enzyme activation is expected if $K_{m,NAD^+,app}$ can be decreased relative to $K_{m,NAD^+}$ - i.e., if the sensitivity of sirtuins to $NAD^+$ can be increased. According to equation (11), $K_{m,NAD^+,app}$ will be smaller than $K_{m,NAD^+}$ if $\frac{K_{d1,A}}{K_{d4,A}} \geq \frac{K_{d1,A}}{K_{d2,A}} \frac{K_{d2,A}}{K_{d3,A}} \frac{K_{d3,A}}{K_{d4,A}} > 1$. To identify mechanisms by which this can occur in terms of the steps in the sirtuin-catalyzed reaction, we consider in turn each of these three respective ratios of $K_{d,A}$'s (or equivalently, the $\Delta\Delta G$'s of the $NAD^+$ binding, exchange, and NAM binding reactions as implied by equation (8)) induced by A binding.

According to equation (13), $K_{d1,A} / K_{d2,A} < 1$ would imply that A binding increases the binding affinity of NAD+ to the E.Ac-Pr complex. This is biophysically implausible for mechanism-based activation; when dissociation constants for substrates decrease upon small molecule binding, this typically occurs through an allosteric mechanism. Thus, we assume that for a mechanism-based activator, $K_{d1,A} \geq K_{d2,A}$. Hence in order to have $K_{m,NAD^+,app} < K_{m,NAD^+}$, we require $\frac{K_{d2,A}}{K_{d3,A}} \frac{K_{d3,A}}{K_{d4,A}} > \frac{K_{d1,A}}{K_{d2,A}}$ or equivalently, according to

(8), $\frac{K_{d,NAM}'}{K_{ex}'}\frac{K_{ex}}{K_{d,NAM}} > \frac{K_{d,NAD+}'}{K_{d,NAD+}}$. The decrease in $K_{m,NAD^+}$ can hence be due to modulation of the exchange rate constants that induces a decrease in $K_{ex}$, an increase in $K_{d,NAM}$, or both. We assume $K_{d,NAM}' \geq K_{d,NAM}$ $(K_{d3,A} \geq K_{d4,A})$ for reasons analogous to those for $K_{d,NAD^+}$ (NAM being the nicotinamide moiety of NAD+). This corresponds to mixed noncompetitive inhibition [29] of base exchange.

As we have previously shown [29], the nicotinamide moiety of $NAD^+$ engages in nearly identical interactions with the enzyme before and after bond cleavage. The salient difference is a conformational change in a conserved phenylalanine side chain (e.g., Phe33 in Sir2Tm, Phe157 in SIRT3) that destabilizes NAM binding after bond cleavage [32, 33]. Since NAM binding is already destabilized by the native protein conformation in this way, and since $\Delta\Delta G_{bind,NAD+}$ induced by the modulator will generally be greater in magnitude than $\Delta\Delta G_{bind,NAM}$ due to disruption of additional contacts between the ADPR moiety of $NAD^+$ and the enzyme, $\frac{K_{d2,A}}{K_{d3,A}}$ is likely to make the dominant contribution to $\frac{K_{d2,A}}{K_{d4,A}}$. Note that there is ample scope for modulation $\Delta G_{ex}$ by the modulator due to the endothermicity of the nicotinamide cleavage reaction (exothermicity of the base exchange reaction). For example, $\Delta G_{ex}$ for Sir2Tm has been calculated to be -4.98 kcal/mol [26]. For comparison, $\Delta G_{bind,NAM}$ for Sir2Af2 was estimated to be -4.1 kcal/mol [30] and $\Delta G_{bind,NAM}$ for SIRT3 was estimated to be <= -3.2 kcal/mol [29]. Taken together, these observations suggest that $\frac{K_{d2,A}}{K_{d3,A}} > \frac{K_{d3,A}}{K_{d4,A}}$ and that the value of $\frac{K_{d2}}{K_{d4}}$ required for activation is likely to be achieved primarily by altering the free energy change of the nicotinamide cleavage reaction. However, our model accommodates the possibility of arbitrary combinations of $\Delta\Delta G_{ex}$ and $\Delta\Delta G_{bind,NAM}$ contributing to activation.

Thus, we find that the following thermodynamic conditions on the binding of A to the various complexes in the sirtuin reaction mechanism are physically plausible and conducive to mechanism-based activation:

$$\begin{aligned} &K_{d1,A} \leq K_{d2,A} \Leftrightarrow K_{d,NAD+}' \geq K_{d,NAD+} \\ &K_{d2,A} >> K_{d3,A} \Leftrightarrow K_{ex}' \ll K_{ex}, \\ &K_{d3,A} \geq K_{d4,A} \Leftrightarrow K_{d,NAM}' \geq K_{d,NAM} \end{aligned} \qquad (17)$$

where the >> sign signifies that $\frac{K_{d2,A}}{K_{d3,A}} > \frac{K_{d3,A}}{K_{d4,A}}$.

Finally, in our original model for sirtuin kinetics in Fig. 3, we assumed that both $K_{d,NAM}$'s– namely, those for dissociation of NAM from E.Ac-Pr.NAM and E.ADPR-Pr-Im.NAM – are roughly equal. We maintain this condition in the presence of A binding, which is reasonable given that A is assumed to not interact

directly with the peptide or ADPR moiety, and since NAM binding does not rely on interactions with the flexible cofactor binding loop [25, 28]. Hence, we have:

$$\frac{[E.ADPR-\mathrm{Pr}-\mathrm{Im}][\mathrm{NAM}]}{[E.ADPR-\mathrm{Pr}-\mathrm{Im}.NAM]} \approx \frac{[E.Ac-\mathrm{Pr}][\mathrm{NAM}]}{[E.Ac-\mathrm{Pr}.NAM]} \Leftrightarrow K_{d5,A} \approx \frac{K_{d1,A}K_{d3,A}}{K_{d4,A}} \qquad (18)$$

Returning to equation (11) for $K_{m,NAD^+,app}$ and substituting $\frac{1+[A]/K_{d2,A}}{1+[A]/K_{d1,A}} \geq 1$, the rapid equilibrium assumptions applied to the present system imply that in order to activate the enzyme at [NAM]=0, A must increase $k_1$ ($k_{1,app}>k_1$), $k_{ex}$ ($k_{ex,app}>k_{ex}$) or both. The rapid equilibrium segments model is not able to distinguish between these scenarios, but given that A is prone to increase $K_{d,NAD^+,app}$, assuming that it also increases $k_1$ is physically implausible. An increase in $k_{ex}$ implies acceleration of the rate of nicotinamide cleavage. In the rapid equilibrium segments framework, this occurs through preferential stabilization of the E.ADPR-Pr-Im complex. Note that across all sirtuins studied, nicotinamide cleavage induces structural changes (for example, unwinding of a helical segment in the flexible cofactor binding loop [34, 35] ) and such changes might enable preferential stabilization of the E.ADPR-Pr-Im complex, in a manner similar to the stabilization of specific loop conformations by mechanism-based inhibitors [17]. We discuss below the biophysical underpinnings whereby an increase in a forward rate constant could be achieved through preferential stabilization of the intermediate complex.

We now consider the effects of binding of a modulator A that satisfies the above requirements for activation on the remaining steady state constants.

- $\alpha_{app}$ : According to equation (12), the aforementioned requirement for activation that $\frac{K_{d2,A}}{K_{d4,A}} \geq \frac{K_{d1,A}}{K_{d4,A}}$ implies a significant increase in $\alpha$ by a factor that will generally exceed $\frac{K_{m,NAD+}}{K_{m,\mathrm{NAD}+,\mathrm{app}}}$ .

- $K_{3,app}$ : According to equation (14), in the presence of such a mechanism-based activator, $K_3$ is expected to increase by a factor similar to that for $\alpha$ under the rapid equilibrium segments approximation. This can occur due to an increase in $K_{d,NAM}$, decrease in $K_{ex}$,or both. Decrease in $K_{ex}$ corresponds to hyperbolic (or partial) noncompetitive inhibition [29] of base exchange/activation of nicotinamide cleavage. With an additional increase in $K_{d,NAM}$, noncompetitive inhibition of base exchange becomes mixed noncompetitive inhibition of base exchange. Additional information (e.g., from high [NAM] initial rate experiments, which permit estimation of $K_{d,NAM,\mathrm{app}}$) is required to separate these possible causes.

- $K_{2,app}$ : With conditions (17), equation (14) predicts a small increase in $K_2$ since $K_{d5,A} > K_{d1,A}$. $K_2$ increases to a smaller extent than $K_3$.

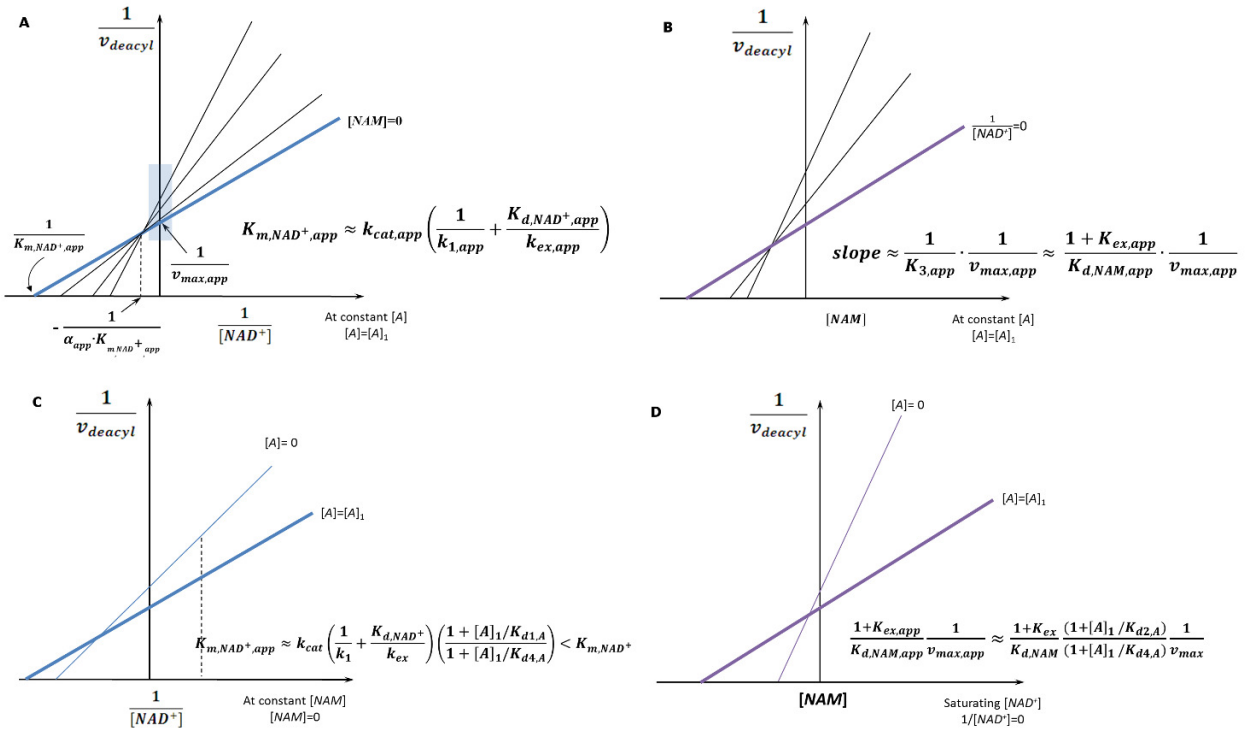


**Figure 4. Mechanism-based activation of sirtuin enzymes: predicted steady-state properties and dose-response behavior.** (a) Double reciprocal plots for deacylation initial rate measurements in the presence of activator. The blue box on the y-axis highlights the data that is used to construct the Dixon plot at saturating [*NAD*$^+$] depicted in (b). (b) Dixon plots for deacylation initial rate measurements in the presence of activator. (c) Comparison of double reciprocal plots at [NAM] = 0 μM in the presence and absence of activator. The dotted line represents a selected value of [NAD$^+$] (e.g., a physiological concentration) at which the extent of activation is assessed. (d) Comparison of Dixon plots at 1/[NAD$^+$] = 0 in the presence and absence of activator. **"**A" denotes a mechanism-based sirtuin activating compound.

- $K_{1,app}$ : With conditions (17), equation (16) predicts an increase in $K_1$.

Fig. 4 depicts the model-predicted changes to the various steady state, Michaelis and dissociation constants in the sirtuin reaction mechanism in the presence of such a modulator.

*Potential means of increasing $k_{ex}$*

From the standpoint of chemical mechanisms of activation, the theory presented raises the important question of how the nicotinamide cleavage rate $k_{ex}$ of sirtuins can be accelerated by a ligand that binds to the various complexes in the deacylation reaction with the specified relative affinities, as predicted by equation (11). It is important to note in this regard that the nicotinamide cleavage reaction in sirtuins is generally believed to be endothermic, which enables effective NAM inhibition of the reaction [26, 36]. Unlike exothermic reactions, stabilization of products in endothermic reactions can decrease the activation barrier for the forward reaction, due to the fact that the transition state resembles the products more than the reactants. The energetics of this reaction, including the role of protein conformational changes, are being studied computationally in our group for mammalian sirtuins.

*Experimental demonstration of mechanism-based sirtuin activation*

In this Section we demonstrate the existence of sirtuin-activating compounds that display all of the characteristics predicted above for mechanism-based activators, providing compelling evidence that they operate according to the prescribed mechanism.

Dihydropyridines (DHPs) constitute a class of compounds with drug-like properties that have been used to target calcium channels, among other proteins and associated disorders [37]. Selected DHPs have been reported to activate multiple sirtuins (SIRT1, SIRT2, and SIRT3) at [NAM]=0 [38], whereas others are inhibitory. The mechanism of action by which DHPs activate sirtuins is unknown, and no approaches have been proposed to interrogate this mechanism. We sought to identify their mechanism of action through application of the theory presented in this paper. For this study we used N-Benzyl-3,5-dicarbethoxy-4-phenyl-1,4-dihydropyridine (DHP-1; Fig. 5) [38]. Initial deacylation rates at the activator's EC1.5 (concentration at which activity is increased by 50% under specified conditions) were measured at varying [NAD+] and [NAM] and the mechanism-based activation as described in Methods. Figs. 6 and 7 depicts the initial rate data at this concentration and in the absence of DHP-1 in a format analogous to the model predictions in Fig. 5a and b, respectively, whereas Fig. 8 presents the dose-response properties of the DHP in a format analogous to Figs.5c and d. Table 1 presents the results of model fitting with the associated values of the initial rate parameters.

These results can now be analyzed in the context of the mechanism-based activation theory presented. In particular, we compare the observed changes in the initial rate parameters $v_{\max}, K_{m,NAD+}, \alpha, K_2, K_3$ at 50 μM concentration (the EC1.5 of this DHP for SIRT3) to those predicted by the theory. The following points should be noted:

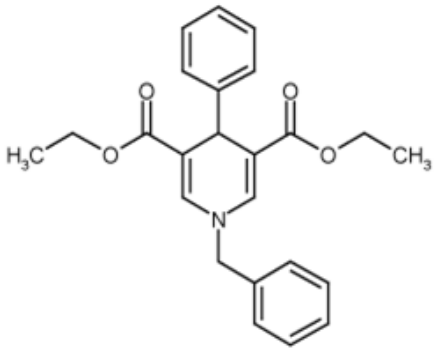


**Figure 5. Sirtuin activator** N-Benzyl-3,5-dicarbethoxy-4-phenyl-1,4-dihydropyridine (DHP-1).

-The negligible change in $v_{\max}$ supports the small $k_{cat}$ approximation according to equation (10).

-As expected from a mechanism-based sirtuin activator that decreases $K_{m,NAD+}$ without changing $v_{\max}$, the slopes of the double reciprocal plots decrease in the presence of activator but the y-intercepts remain nearly the same.

-Moreover, the increase in $\alpha$ by a factor that exceeds the decrease in $K_{m,NAD+}$ indicates that $K_{d,NAD+}$ is increased by DHP-1 binding (i.e., that DHP-1 induces some level of competitive inhibition of deacetylation by destabilizing the native binding mode of NAD+; see equations (11-13)).

-The slight increase in $K_{2,app}$ relative to $K_2$ is to be expected based on the discussion following equation (15).

It is also possible to carry out analogous experiments at saturating [DHP-1], due to the plateau in activity predicted by equations (10) and (11), in order to obtain estimates of the modulated steady state parameters in the presence of bound A (i.e., those corresponding to the back face of Fig. 3), rather than the apparent constants. Based on the value of $K_3'$, we can estimate $\Delta\Delta G_{24}$, namely the change in the free energy gap between $E.ADPR - Ac - \mathrm{Im}$ and $E.Ac - \mathrm{Pr}.\mathrm{NAD}^+$, using equation (14) with saturating [A] (or equivalently, equation (8)).

Separately, initial rate measurements were carried out at nonsaturating [Ac-Pr] and saturating [$NAD^+$], in order to further explore whether the modulator can activate the enzyme by decreasing the $K_{d,Ac\text{-}Pr}$ of the peptide substrate, as in the case of allosteric activators. No significant rate enhancement was observed (data not shown), as expected. This lack of activation at saturating [NAD+] is consistent with the predictions of the theory. The fact that DHP-1 also activates SIRT1 and SIRT2 is also consistent with the generality of mechanism-based activation.

The demonstrated ability to relate the modulated steady state kinetics of the enzyme to the manner in which the activator interacts with the various species in the reaction mechanism stands in sharp contrast with the vast majority of, if not all, previously characterized enzyme activators [9]. Having identified a mechanism-based activator that displays the qualitative features identified above under the rapid equilibrium segments approximation, we can now subject the saturated DHP system to base exchange initial rate experiments in addition to deacylation initial rate experiments [36, 39, 40], which will together enable estimation of all the rate constants $k_1'$, $k_{-1}'$, $k_2'$, $k_{-2}'$, $k_{ex}'$, $k_{-ex}'$, $k_{cat}'$. This will elucidate the mechanism of DHP-induced activation in more detail than would be possible in a rapid equilibrium framework (i.e., in terms of the 7 rate constants instead of 5 $K_{d,A}$'s) and will be carried out in future work, along with additional structural and biophysical characterization.

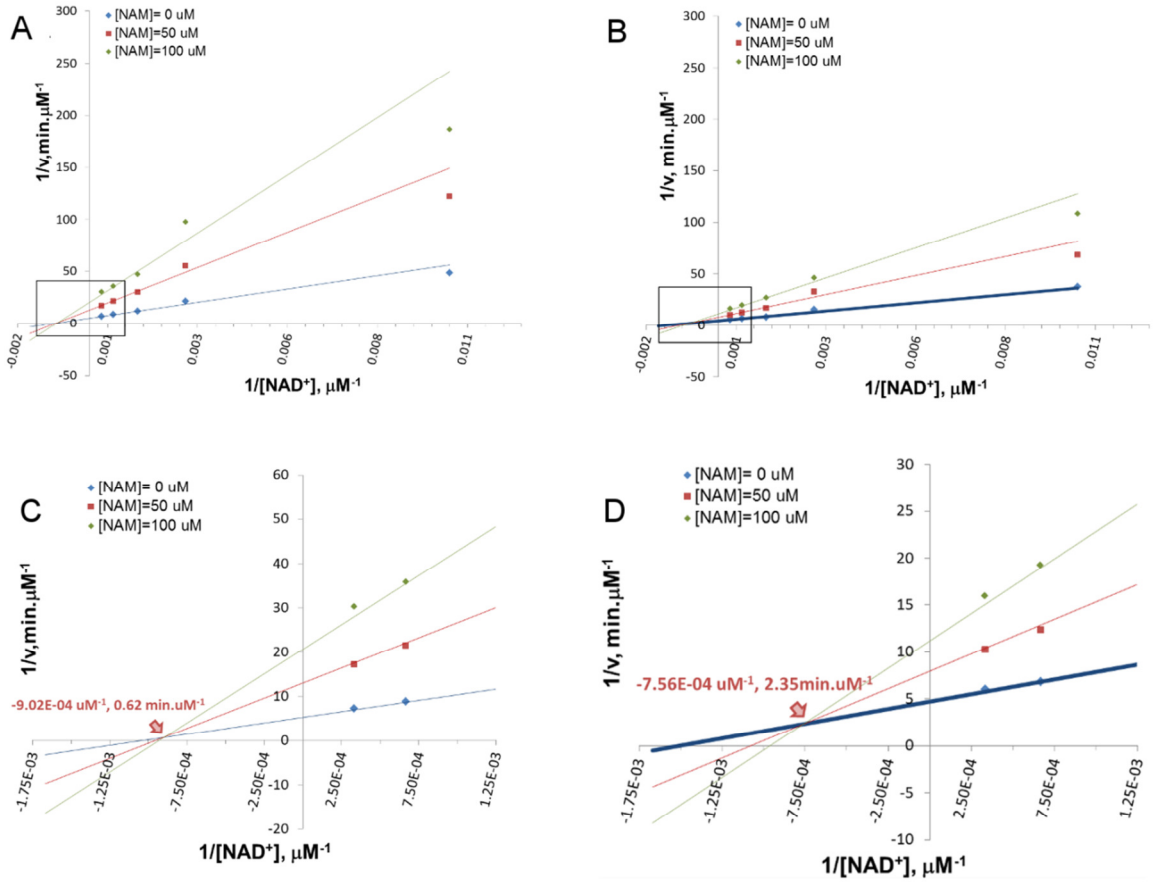


**Figure 6. Mechanism-based activation of SIRT3 by a dihydropyridine derivative: steady-state [NAD+] response at selected [NAM].** Recombinant human SIRT3 was incubated for 0, 5, 10, 20, 30, 60, and 120 min at 37°C in the presence of 100, 375, 750, 1500, 3000 μM $NAD^+$ and 0, 50, 100 μM NAM. (a) Double reciprocal plots for deacylation initial rate experiments in the presence of inhibitor (NAM) with 0μM DHP-1. (b) Double reciprocal plots for deacylation initial rates in the presence of NAM with 50μM ($EC_{1.5}$) of DHP-1. (c,d) Magnifications of the points of intersection for a),b) respectively; the physical interpretation of the change in position of this point induced by modulator is provided by Fig. 4a and equation (6).

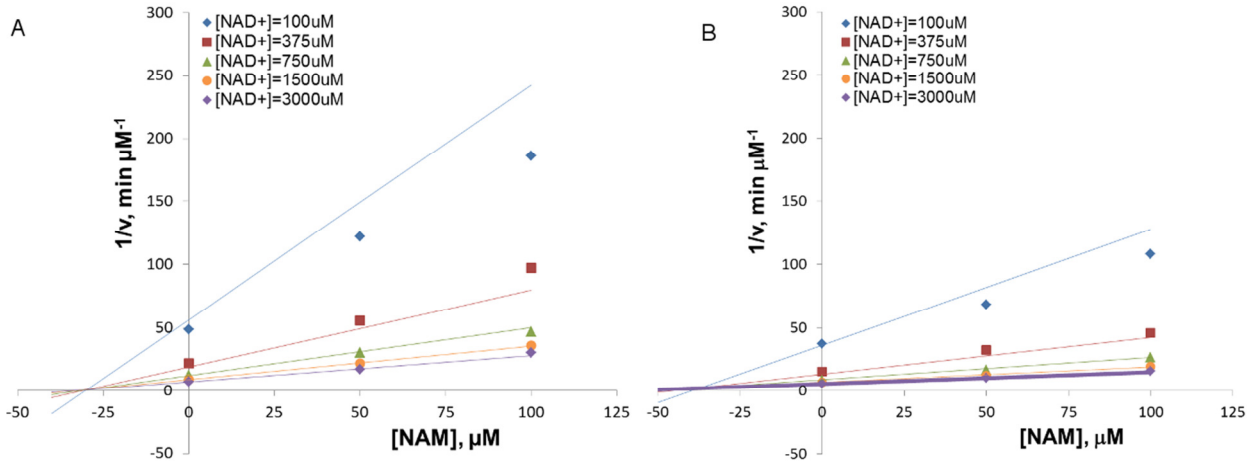


**Figure 7. Mechanism-based activation of SIRT3 by a dihydropyridine derivative: steady-state [NAM] response at selected [NAD+].** Recombinant human SIRT3 was incubated for 0, 5, 10, 20, 30, 60, and 120 min at 37°C in the presence of 100, 375, 750, 1500, 3000 μM $NAD^+$ and 0, 50, 100 μM NAM. (a) Dixon plots for deacylation initial rates in the presence of NAM with 0μM DHP-1 for different concentrations of $NAD^+$. (b) Dixon plots for deacylation initial rates in the presence of NAM with 50μM DHP-1 ($EC_{1.5}$) for different concentrations of $NAD^+$.

## Discussion

We have presented a model for activation of sirtuin enzymes suitable for the design and characterization of mechanism-based sirtuin activating compounds (MB-STACs) that can in principle activate any of the mammalian sirtuins SIRT1-7, unlike previously proposed strategies for sirtuin activation. Also, the activation model presented herein should be applicable to any substrate, unlike previously reported allosteric activation of SIRT1 that was found to accelerate deacylation for only a small fraction of over 6000 physiologically relevant peptide substrates studied, due to the need for "substrate-assistance" in the allosteric mechanism [13]. Moreover, this framework comprises a new mode of enzyme activation that is distinct from any of the four modes of activation previously known across all families of enzymes.

Using this modeling framework, we have shown how modulation of $K_{m,NAD^+}$ independently of $K_{d,NAD^+}$ can increase the activity of sirtuins at [NAM]=0 in a manner that mimics the effects of $NAD^+$ supplementation [41] but in a selective fashion. This activation also applies at nonzero [NAM], decreasing the sensitivity of the sirtuin to physiological NAM inhibition in addition to increasing its sensitivity to physiological NAD+. These predictions have been validated through an experimental example of mechanism-based sirtuin activation. Such mechanism-based sirtuin activation has advantages over a) allosteric activation, which is only possible for SIRT1, is substrate-dependent, and cannot fully compensate for the reduction in $NAD^+$ levels that is responsible for many aspects of health decline during organismic aging [11, 12, 42]; b) activation of the $NAD^+$ biosynthetic enzyme Nampt [43], which regenerates $NAD^+$ from NAM and hence has nonselective effects on all enzymes that use an $NAD^+$ cofactor; and c) inhibition of $NAD^+$-dependent PARP enzymes, which consume $NAD^+$ but are required to repair DNA damage [22]. Moreover, it has the potential to enable isoform-specific sirtuin enzyme activation.

**Table 1.** Model parameter estimates from global nonlinear fitting of equation (2) for SIRT3 in the presence and absence of DHP-1[1]. The values at 50μM DHP-1 are apparent values.

| Best-fit values | 0 μM DHP-1 | 50 μM DHP-1 |
|---|---|---|
| **Vmax** | 0.1911 | 0.2118 |
| **Alpha** | 1.139 | 1.988 |
| **K2** | 29.81 | 36.93 |
| **Km** | 972.9 | 664.8 |
| **Std. Error** | | |
| **Vmax** | 0.006755 | 0.009142 |
| **Alpha** | 0.3519 | 0.8075 |
| **K2** | 5.727 | 8.83 |
| **Km** | 85.04 | 82 |
| **95% Confidence Intervals** | | |
| **Vmax** | 0.1762 to 0.2059 | 0.1917 to 0.2319 |
| **Alpha** | 0.3646 to 1.913 | 0.2105 to 3.765 |
| **K2** | 17.20 to 42.42 | 17.50 to 56.37 |
| **Km** | 785.7 to 1160 | 484.3 to 845.3 |
| **Goodness of Fit** | | |
| **Degrees of Freedom** | | |
| **R square** | 0.9948 | 0.9869 |
| **Absolute Sum of Squares** | 0.00004819 | 0.0001752 |
| **Sy.x** | 0.00259 | 0.004807 |

The rapid equilibrium segments approximation (Appendix, equation A3) was applied in order to illustrate how a ligand that binds outside the $NAD^+$ binding site can in principle increase sirtuin activity through only modulation of the relative free energies of the various species in the reaction mechanism. More detailed analysis of the mechanism of action of MB-STACs like the dihydropyridines can be achieved by complete kinetic characterization in presence/absence of the activator (e.g., by coupling base exchange with deacylation experiments). Such analyses will shed light on whether mechanism-based sirtuin activation exploits the free energy profile of the sirtuin nicotinamide cleavage and base exchange reactions – and if so, how. Note that, as discussed, the nicotinamide cleavage step is reversible and the DHP activator both decreases the NAM sensitivity of the sirtuin and activates at [NAM]=0. Besides DHPs, it is worthwhile to apply the mechanism identification methodology presented herein to any STACs that may be found to activate either SIRT2-7 or SIRT1-catalyzed reactions on substrates other than those of the limited type identified in [11-13] to which traditional STACs are restricted. The opportunities for mechanism-based activation of mammalian sirtuins will depend on their particular values of $K_{m,NAD^+}$ and the underlying values of the associated rate constants. Importantly, a sirtuin need not be highly sensitive to base exchange inhibition in order to be susceptible to mechanism-based activation.

[1]Enzyme purity can affect absolute magnitudes of kinetic parameters. As discussed, the ratios of apparent parameter values in the presence of activator to their respective values in the absence of activator are the focus of the current study.

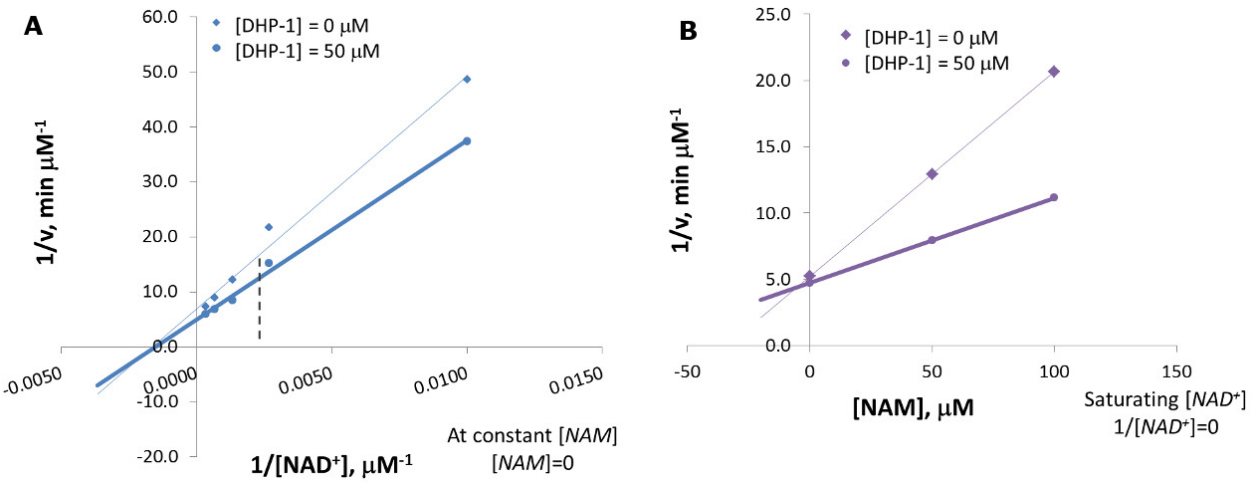


**Figure 8. Mechanism-based activation of SIRT3 by a dihydropyridine derivative: dose-response behavior.** Recombinant human SIRT3 was incubated for 0, 5, 10, 20, 30, 60, and 120 min at 37°C in the presence of 100, 375, 750, 1500, 3000 μM $NAD^+$ and 0, 50, 100 μM NAM. (a) Comparison of double reciprocal plots at [NAM] = 0 μM in the presence and absence of DHP-1. The dotted line corresponds to 375 μM [NAD+], which is within the physiological range. (b) Comparison of Dixon plots at saturating $NAD^+$ in the presence and absence of DHP-1.

Structurally, binding outside of the $NAD^+$ binding site (the so-called A and C pockets [25, 44]) appears to be essential for mechanism-based activation. We are currently exploring prospective binding sites for MB-STACs. Moreover, rational design will require analysis of the relative free energies of complexes depicted in Fig. 3. We have recently initiated computational studies [29] that assess such free energy differences for some of the front face (apo) complexes in this Figure, and further studies are in progress.

The enzyme activation theory presented herein motivates experimental workflows for the hit identification, hit-to-lead evolution, and lead optimization of mechanism-based activators. In particular, the theory enables the identification and evolution of important hits that may be inhibitors, not activators, by decomposing the observed kinetic effects of a modulator into components and identifying those molecules that display favorable values of a subset of these components as hits even if the net effect on catalytic turnover is inhibition. Compared to standard library screening for hit identification and hit-to-lead evolution, this approach allows application of multiobjective optimization techniques (through iterative mutations to functional groups) to sirtuin activator design. Such workflows would be fundamentally different from traditional drug discovery workflows and would bear more similarity to the directed evolution of enzymes. The theory presented also establishes foundations for the rational design of sirtuin-activating compounds, enabling the application of state-of-the-art computational methods to activator design in a manner analogous to computational enzyme design [45]. Finally, it raises the important question as to whether other enzyme families may also be activatable through such a mechanism-based mode of action -- and if so, which families.

## Methods

### *Chemicals and Reagents*

Human recombinant SIRT3 was purchased from Enzo Life Sciences (Farmingdale, NY, USA). The enzyme purity following multistep column chromatography was determined to be ~ 70% by SDS-PAGE. The specific activity of the enzyme was 20U/μg, where one unit will deacetylate 1pmol/min of substrate at 37C, using 500μM substrate and 500μM $NAD^+$. Enzyme concentrations were determined using the method of Bradford with bovine serum albumin (BSA) as the standard. All other chemicals used were of the highest purity commercially available and were purchased from Sigma (St. Louis, MO, USA), Enzo Life Sciences (Farmingdale, NY, USA), and Fisher Scientific (Pittsburgh, PA, USA).

### *Measurement of Deacetylation Activity Using a Fluorolabeled Peptide*

The steady state parameters and catalytic efficiency ($k_{cat}/K_m$) of deacetylase activity of recombinant human SIRT3 were determined using a fluorometric assay. The deacetylation activities were measured by using the SIRT3 Fluorimetic Drug Discovery Kit (AK 557, Enzo Life Sciences). This assay system allows detection of a fluorescent signal upon deacetylation of an acetylated substrate peptide, comprising amino acids 317–320 of human p53 (Gln-Pro-Lys-LysAc) for SIRT3, when treated with developer. The intensity of fluorescence was measured on a multifunctional microplate reader (TECAN Infinite M200 PRO, Switzerland, Tecan Group Ltd.) with excitation set at 355 nm and emission detection set at 455 nm. The initial rate of the $NAD^+$ - dependent deacetylation activity of SIRT3 enzyme was measured at different concentrations of $NAD^+$. The reactions were carried out at $37^0$C in a 50 μl reaction volume containing 50 mM Tris/Cl (pH = 8.0), 137 mM NaCl, and 100 μM fluorolabeled peptide substrate. The raw data were fitted to the Michaelis-Menten equation and defined inhibition models by using GraphPad Prism (GraphPad Software, Inc, CA) to obtain the kinetic constants. Fluorimetric assays of sirtuin activity have been shown to provide results comparable to those from assays using unmodified peptides in studies of nonallosteric modulators. In assays of allosteric modulators – which are not considered in the present work – artifacts reported in the presence of the fluorescent label were later shown to occur due to the hydrophobic fluorophore participating in the modulator's allosteric activation mechanism.

### *Measurement of EC1.5 Values for SIRT3 Activator DHP-1*

EC1.5, is the effective concentration able to increase the enzyme activity of 150%. This assay was used to measure the potency of activation of SIRT3 by DHP1c. All reagents are diluted on ice in the following reaction buffer: 50 mM Tris/Cl, pH 8.0, 137 mM NaCl, 2.7 mM KCl, 1 mM $MgCl_2$, and 1 mg/mL BSA. Thus for each reaction well, 5U of SIRT3 enzyme is added to 500 μM $NAD^+$, 250 μM fluorolabeled peptide substrate, and DHP1c of interest at a given concentration (0-100uM) in a total reaction volume of 50 μL. After an hour incubation at 37 $^o$C, the reaction is stopped upon addition of 1X Developer for a final reaction volume of 100 μL. The reaction is incubated at 37 $^o$C for an additional 15 min and then read on the plate reader. Positive controls contained only enzyme, substrate, $NAD^+$, and DMSO while background controls contained substrate, $NAD^+$, and DMSO only.

*Measurement of the Activation Effect of DHP-1 on SIRT3 in the presence of NAM*

The deacetylation activity was measured by using the SIRT3 Fluorimetric Drug Discovery Kit (AK 557, Enzo Life Sciences). In the presence of 50μM of NAM, deacetylation activity of SIRT3 enzyme was measured under addition of different concentrations of DHP-1, range from 0 μM to 50 μM. The reactions were carried out at $37^0$C in a 50 μl reaction volume containing 50 mM Tris/Cl (pH= 8), 137 mM NaCl, and 100 μM fluorolabeled peptide substrate.

Appendix

Expressions for $c_{ij}$'s in equation (1):

$$
\begin{aligned}
c_{11} &= k_{cat}k_{-2}\left[k_{cat}k_{ex} + k_{cat}k_{-1} + k_{ex}k_{-2} + k_{-1}k_{-2} + k_{-ex}k_{-1}\right] \\
c_{12} &= k_2k_{-ex}k_{-1}k_{-2} + k_{cat}\left(k_{ex}k_{-2}k_2 + k_{-1}k_{-2}k_2\right) \\
\\
c_{21} &= k_{cat}\left(k_{-2}k_1k_{cat} + k_{-2}k_1k_{-2} + k_{-2}k_1k_{-ex}\right) \\
c_{22} &= k_1k_2k_{-ex}k_{-2} + k_{cat}k_1k_2k_{-2} \\
\\
c_{31} &= k_{cat}k_1k_{ex}k_{-2} \\
c_{32} &= k_1k_{ex}k_2k_{-2} \\
\\
c_{41} &= k_1k_{ex}k_{-2}k_{-2} \\
\\
c_{51} &= k_{cat}k_1k_{ex}k_{cat} \\
c_{52} &= k_{cat}\left(k_{cat}k_2k_{ex} + k_{cat}k_{-1}k_2 + k_{-2}k_2k_{ex} + k_{-2}k_{-1}k_2 + k_{-ex}k_{-1}k_2\right) \\
c_{53} &= k_{cat}k_1k_{ex}k_2 \\
c_{54} &= k_{-ex}k_{-1}k_2k_2 + k_{cat}\left(k_{ex}k_2k_2 + k_{-1}k_2k_2\right)
\end{aligned}
\qquad \text{(A1)}
$$

With these, the expressions for the steady state constants in equation (3) follow from

$$
\begin{aligned}
v_{\max} &= \frac{k_{cat}\left(c_{31}+c_{41}\right)}{c_{21}+c_{31}+c_{41}+c_{51}}[E]_0 \\
K_{m,NAD^+} &= \frac{c_{11}}{c_{21}+c_{31}+c_{41}+c_{51}} \\
\frac{1}{K_1} &= \frac{c_{32}}{c_{31}+c_{41}} \\
\frac{1}{K_2} &= \frac{1}{K_{m,\mathrm{NAD}^+}}\frac{c_{12}+c_{52}}{c_{21}+c_{31}+c_{41}+c_{51}} \\
\frac{1}{K_{2'}} &= \frac{1}{K_{m,\mathrm{NAD}^+}}\frac{c_{54}}{c_{21}+c_{31}+c_{41}+c_{51}} \\
\frac{1}{K_3} &= \frac{c_{22}+c_{32}+c_{53}}{c_{21}+c_{31}+c_{41}+c_{51}}
\end{aligned}
\qquad (\mathrm{A}\,2)
$$

The rapid equilibrium segments expressions for the steady-state concentrations of the species in the sirtuin reaction mechanism depicted in Fig. 3 are:

$$
\begin{aligned}
&[E.Ac-\mathrm{Pr}]/[E.Ac-\mathrm{Pr}]_0 \approx c_{11}+c_{12}[\mathrm{NAM}] \\
&[E.Ac-\mathrm{Pr}.\mathrm{A}]/[E.Ac-\mathrm{Pr}]_0 \approx \frac{[A]}{K_{d1,A}}\left(c_{11}+c_{12}[\mathrm{NAM}]\right) \\
&[E.Ac-\mathrm{Pr}.\mathrm{NAD}^+]/[E.Ac-\mathrm{Pr}]_0 \approx c_{21}[NAD^+]+c_{22}[\mathrm{NAD}^+][\mathrm{NAM}] \\
&[E.Ac-\mathrm{Pr}.\mathrm{NAD}^+.\mathrm{A}]/[E.Ac-\mathrm{Pr}]_0 \approx \frac{[A]}{K_{d2,A}}\left(c_{21}[NAD^+]+c_{22}[\mathrm{NAD}^+][\mathrm{NAM}]\right) \\
&[E.ADPR-Ac-\mathrm{Im}.NAM]/[E.Ac-\mathrm{Pr}]_0 \approx c_{31}[NAD^+]+c_{32}[NAD^+][NAM] \\
&[E.ADPR-Ac-\mathrm{Im}.NAM.\mathrm{A}]/[E.Ac-\mathrm{Pr}]_0 \approx \frac{[A]}{K_{d3,A}}\left(c_{31}[NAD^+]+c_{32}[NAD^+][NAM]\right) \\
&[E.ADPR-Ac-\mathrm{Im}]/[E.Ac-\mathrm{Pr}]_0 \approx c_{41}[\mathrm{NAD}^+] \\
&[E.ADPR-Ac-\mathrm{Im}.\mathrm{A}]/[E.Ac-\mathrm{Pr}]_0 \approx \frac{[A]}{K_{d4,A}}\left(c_{41}[\mathrm{NAD}^+]\right) \\
&[E.\mathrm{Ac}-\mathrm{Pr}.NAM]/[E.Ac-\mathrm{Pr}]_0 \approx c_{51}[NAD^+]+c_{52}[NAM]+\mathrm{c}_{53}[\mathrm{NAD}^+][\mathrm{NAM}] \\
&[E.\mathrm{Ac}-\mathrm{Pr}.NAM.\mathrm{A}]/[E.Ac-\mathrm{Pr}]_0 \approx \frac{[A]}{K_{d5,A}}\left(c_{51}[NAD^+]+c_{52}[NAM]+\mathrm{c}_{53}[\mathrm{NAD}^+][\mathrm{NAM}]\right)
\end{aligned}
\qquad (A3)
$$

## References


1. Kaeberlein M, McVey M, & Guarente L (1999) The SIR2/3/4 complex and SIR2 alone promote longevity in Saccharomyces cerevisiae by two different mechanisms. *Genes & Development* 13(19):2570-2580.
2. Hirsch BM & Zheng W (2011) Sirtuin mechanism and inhibition: explored with N(epsilon)-acetyl-lysine analogs. *Molecular bioSystems* 7(1):16-28.
3. Cen Y (2010) Sirtuins inhibitors: the approach to affinity and selectivity. *Biochimica et biophysica acta* 1804(8):1635-1644.
4. Sauve AA (2010) Sirtuin chemical mechanisms. *Biochimica Et Biophysica Acta-Proteins and Proteomics* 1804(8):1591-1603.
5. Hu P, Wang S, & Zhang Y (2008) Highly dissociative and concerted mechanism for the nicotinamide cleavage reaction in Sir2Tm enzyme suggested by ab initio QM/MM molecular dynamics simulations. *Journal of the American Chemical Society* 130(49):16721-16728.
6. Zhou Y, *et al.* (2012) The bicyclic intermediate structure provides insights into the desuccinylation mechanism of human sirtuin 5 (SIRT5). *The Journal of biological chemistry* 287(34):28307-28314.
7. Mercken EM, *et al.* (2014) SRT2104 extends survival of male mice on a standard diet and preserves bone and muscle mass. *Aging Cell* 13(5):787-796.
8. Mitchell SJ, *et al.* (2014) The SIRT1 activator SRT1720 extends lifespan and improves health of mice fed a standard diet. *Cell Rep* 6(5):836-843.
9. Zorn JA & Wells JA (2010) Turning enzymes ON with small molecules. *Nat Chem Biol* 6(3):179-188.
10. Sinclair DA & Guarente L (2014) Small-molecule allosteric activators of sirtuins. *Annual review of pharmacology and toxicology* 54:363-380.
11. Hubbard BP, *et al.* (2013) Evidence for a Common Mechanism of SIRT1 Regulation by Allosteric Activators. *Science* 339(6124):1216-1219.
12. Dai H, *et al.* (2015) Crystallographic structure of a small molecule SIRT1 activator-enzyme complex. *Nat Commun* 6:7645.
13. Lakshminarasimhan M, Rauh D, Schutkowski M, & Steegborn C (2013) Sirt1 activation by resveratrol is substrate sequence-selective. *Aging (Albany NY)* 5(3):151-154.
14. North BJ, *et al.* (2014) SIRT2 induces the checkpoint kinase BubR1 to increase lifespan. *Embo Journal* 33(13):1438-1453.
15. Brown K, *et al.* (2013) SIRT3 reverses aging-associated degeneration. *Cell Rep* 3(2):319-327.
16. Kanfi Y, *et al.* (2012) The sirtuin SIRT6 regulates lifespan in male mice. *Nature* 483(7388):218-221.
17. Gertz M, *et al.* (2013) Ex-527 inhibits Sirtuins by exploiting their unique NAD(+)-dependent deacetylation mechanism. *Proceedings of the National Academy of Sciences of the United States of America* 110(30):E2772-E2781.
18. Rumpf T, *et al.* (2015) Selective Sirt2 inhibition by ligand-induced rearrangement of the active site. *Nat Commun* 6:6263.
19. Gomes AP, *et al.* (2013) Declining NAD(+) induces a pseudohypoxic state disrupting nuclear-mitochondrial communication during aging. *Cell* 155(7):1624-1638.
20. Qin WP, *et al.* (2006) Neuronal SIRT1 activation as a novel mechanism underlying the prevention of Alzheimer disease amyloid neuropathology by calorie restriction. *Journal of Biological Chemistry* 281(31):21745-21754.
21. Satoh A & Imai S (2014) Systemic regulation of mammalian ageing and longevity by brain sirtuins. *Nat Commun* 5:4211.
22. Massudi H, *et al.* (2012) Age-Associated Changes In Oxidative Stress and NAD(+) Metabolism In Human Tissue. *Plos One* 7(7):e42357.
23. Canto C, *et al.* (2012) The NAD(+) precursor nicotinamide riboside enhances oxidative metabolism and protects against high-fat diet-induced obesity. *Cell Metab* 15(6):838-847.
24. Smith BC & Denu JM (2007) Sir2 deacetylases exhibit nucleophilic participation of acetyl-lysine in NAD+ cleavage. *Journal of the American Chemical Society* 129(18):5802-5803.
25. Avalos JL, Boeke JD, & Wolberger C (2004) Structural basis for the mechanism and regulation of Sir2 enzymes. *Molecular Cell* 13(5):639-648.
26. Liang Z, *et al.* (2010) Investigation of the catalytic mechanism of Sir2 enzyme with QM/MM approach: SN1 vs SN2? *The journal of physical chemistry. B* 114(36):11927-11933.

27. Shi YW, Zhou YZ, Wang SL, & Zhang YK (2013) Sirtuin Deacetylation Mechanism and Catalytic Role of the Dynamic Cofactor Binding Loop. *J. Phys. Chem. Lett.* 4(3):491-495.
28. Avalos JL, Bever KM, & Wolberger C (2005) Mechanism of sirtuin inhibition by nicotinamide: Altering the NAD(+) cosubstrate specificity of a Sir2 enzyme. *Molecular Cell* 17(6):855-868.
29. Guan X, Lin P, Knoll E, & Chakrabarti R (2014) Mechanism of inhibition of the human sirtuin enzyme SIRT3 by nicotinamide: computational and experimental studies. *PLoS One* 9(9):e107729.
30. Cen Y & Sauve AA (2010) Transition state of ADP-ribosylation of acetyllysine catalyzed by Archaeoglobus fulgidus Sir2 determined by kinetic isotope effects and computational approaches. *Journal of the American Chemical Society* 132(35):12286-12298.
31. Sauve AA, Moir RD, Schramm VL, & Willis IM (2005) Chemical activation of Sir2-dependent silencing by relief of nicotinamide inhibition. *Molecular Cell* 17(4):595-601.
32. Hawse WF*, et al.* (2008) Structural Insights Into Intermediate Steps in the Sir2 Deacetylation Reaction. *Structure* 16(9):1368-1377.
33. Armstrong CM, Kaeberlein M, Imai SI, & Guarente L (2002) Mutations in Saccharomyces cerevisiae gene SIR2 can have differential effects on in vivo silencing phenotypes and in vitro histone deacetylation activity. *Mol Biol Cell* 13(4):1427-1438.
34. Szczepankiewicz BG*, et al.* (2012) Synthesis of carba-NAD and the structures of its ternary complexes with SIRT3 and SIRT5. *The Journal of organic chemistry* 77(17):7319-7329.
35. Zhao KH, Harshaw R, Chai XM, & Marmorstein R (2004) Structural basis for nicotinamide cleavage and ADP-ribose transfer by NAD(+)-dependent Sir2 histone/protein deacetylases. *Proceedings of the National Academy of Sciences of the United States of America* 101(23):8563-8568.
36. Sauve AA & Schramm VL (2003) Sir2 regulation by nicotinamide results from switching between base exchange and deacetylation chemistry. *Biochemistry* 42(31):9249-9256.
37. Hockerman GH, Peterson BZ, Johnson BD, & Catterall WA (1997) Molecular determinants of drug binding and action on L-type calcium channels. *Annual review of pharmacology and toxicology* 37:361-396.
38. Mai A*, et al.* (2009) Study of 1,4-dihydropyridine structural scaffold: discovery of novel sirtuin activators and inhibitors. *J Med Chem* 52(17):5496-5504.
39. Jackson MD, Schmidt MT, Oppenheimer NJ, & Denu JM (2003) Mechanism of nicotinamide inhibition and transglycosidation by Sir2 histone/protein deacetylases. *The Journal of biological chemistry* 278(51):50985-50998.
40. Sauve AA & Schramm VL (2003) Nicotinamide inhibition of SIR2 is a consequence of chemical competition for an ADPR - peptidyl intermediate. *Biochemistry* 42(28):8630-8630.
41. Imai S (2010) A possibility of nutriceuticals as an anti-aging intervention: Activation of sirtuins by promoting mammalian NAD biosynthesis. *Pharmacological research : the official journal of the Italian Pharmacological Society* 62(1):42-47.
42. Pacholec M*, et al.* (2010) SRT1720, SRT2183, SRT1460, and Resveratrol Are Not Direct Activators of SIRT1. *Journal of Biological Chemistry* 285(11):8340-8351.
43. Wang G*, et al.* (2014) P7C3 neuroprotective chemicals function by activating the rate-limiting enzyme in NAD salvage. *Cell* 158(6):1324-1334.
44. Hawse WF & Wolberger C (2009) Structure-based Mechanism of ADP-ribosylation by Sirtuins. *Journal of Biological Chemistry* 284(48):33654-33661.
45. Chakrabarti R, Klibanov AM, Friesner RA (2005) Sequence optimization and designability of enzyme active sites. *Proceedings of the National Academy of Sciences of the United States of America* 102: 12035-12040.